Statistical Shape and Intensity Models of the Human Wrist

Thor E. Andreassen[1], Taylor P. Trentadue[1], Andrew R. Thoreson[1], Shuai Leng[1], David R. Holmes III[1], Kristin D. Zhao[1]
[1]Mayo Clinic, Rochester, MN
andreassen.thor@mayo.edu

Disclosures: Thor E. Andreassen (N), Taylor P. Trentadue (N), Andrew R. Thoreson (N), Shuai Leng (N), David R. Holmes III (N), Kristin D. Zhao (N)

INTRODUCTION: Statistical shape modeling (SSM) is a vital tool in many musculoskeletal applications[1]. More recently, SSM has been complemented by the addition of bone radiodensity in the form of statistical intensity models (SIM) to investigate variation in bone shape (SSM) and how density within the bone can vary (SIM)[2]. In addition to conventional applications of SSM, SIM have shown success in 3D bone reconstruction from planar radiographs[3], rapid patient-specific finite element modeling[4], implant design[5], and fracture risk prediction[5]. While most SIM have focused on the lower extremities, these models may be beneficial in the wrist, particularly in the contexts of wrist arthroplasty[6,7] and to investigate mechanisms of and risk factors for distal radius fractures, the second most common fracture location[8]. This work aimed to develop a multi-object SSM and SIM of the radius, ulna, and carpal bones.

METHODS: This work used a dataset of 30 asymptomatic participants (50% F, median age 27 years) imaged using photon-counting detector computed tomography (CT)[9] collected as part of an Institutional Review Board approved study. The static CT volumes included the distalmost phalanges through the distal radial metadiaphysis with a spatial resolution of 0.2 mm. CT volumes were segmented using Analyze (Mayo Foundation for Medical Education and Research, Rochester, MN), exported as 2D meshes (3D triangulated surfaces), and smoothed with a combination of custom code in MATLAB (MathWorks) and publicly-available tools[10,11]. The radius and ulna were cropped proximally to ¾ the distance spanned in the radial-ulnar direction of the wrist from the radial styloid to the central sigmoid notch[12,13]. A participant chosen at random (M, 38 years) was used to generate a set of template meshes[14]. 3D meshes (3D tetrahedral volumetric) were created for each template bone using publicly-available algorithms[11] and then morphed to each participant's 2D bone meshes using an open-source non-linear morphing algorithm[15]. This morphing process resulted in uniform 3D meshes with internally-defined nodes (approximately 50,000 nodes per bone at 20 node/mm^3 on average) for each participant. The CT numbers (Hounsfield units [HU]) for each internal node were mapped from the static CT for each participant using trilinear interpolation. A SSM was created using the Cartesian coordinates and a SIM was created using the HU at the nodes of the 3D meshes. All bones were transformed to the average position of each bone across participants. The explained variances per principal component (PC) were captured for the SSM and SIM, and both were truncated to the minimum number of PC that captured 95% of explained variance. The ratio of volumetric change relative to the mean size for each bone in the SSM was calculated for each PC at ±3 standard deviations. Correlations (r) between the SSM and SIM were calculated to identify patterns in HU for a given shape; a threshold of $r > 0.3$ was used to define a fair or better correlation[16].

RESULTS: The total number of PC to capture 95% of explained variance were 18 and 28 for the SSM and SIM, respectively (**Fig. 1**). Figures demonstrate change in shape for the PC in the SSM and for changing HU for the PC in the SIM. The 1st PC of the SSM had an approximately uniform volumetric scaling factor across all bones of 1.63 (**Fig. 2**). The 2nd PC of the SSM generally had a volumetric scaling factor of 1.36, except the pisiform at 1.69 (**Fig. 2**). The 1st PC of the SIM had an approximately uniform increase or decrease in HU across all bones (**Fig. 3**). When HU was normalized to z-scores based on range of values observed across all participants at each node, the 1st PC primarily impacted the cortical bone. Moderate or higher correlations (range of r: 0.301 – 0.579) were found in 53 pairs (10.5%) of PC between the SSM and SIM.

DISCUSSION: This work developed a SSM and SIM of the wrist using a combination of photon-counting detector CT data—yielding high spatial resolution from a clinical CT system—and a publicly-available morphing algorithm[15]. The SSM was more compact—with greater explained variance for the same number of PC—than the SIM, highlighting that individual differences in HU within bones is more variable than bone shape differences. 10.5% of the pairs of PC between SSM and SIM were found with fair or greater correlations. While some patterns exist between bone shape and HU, most variations are unique. This may be important, as certain pathologies and treatments may affect internal bone density without changing bone shape and vice versa. This work was limited to a relatively small number (n=30) of asymptomatic participants. The multi-object SSM included analyses of changing shapes but not corresponding pose changes, limiting ability to assess articular metrics. The work did not exclude participants with incidental osseous findings, such as enostoses or carpal bosses, which will create outliers and influence extrema as observed in the SIM and SSM. Future work will increase the number of participants and expand to those with diverse pathologies and injury states, ultimately investigating pathology-driven patterns in both SSM and SIM.

SIGNIFICANCE: This novel work investigates patterns in the 3D shape and volumetric distribution of radiodensity of wrist bones amongst asymptomatic individuals, integrating advanced high spatial resolution clinical imaging with publicly-available tools. This work demonstrated that differences in the underlying distribution of bone radiodensity are more variable than shape and, in most cases, these changes are not correlated.

REFERENCES: [1]Cai et al., Intel Med, 2024; [2]Grassi et al., Cur Osteop Rep, 2021; [3]Burton et al., Ann Biomed Eng, 2024; [4]Xu et al., Res Square, 2025; [5]Bryan et al., J Biomech, 2009; [6]Taylor et al., J Wrist Surg, 2024; [7]Eschweiler et al., Life, 2022; [8]Mauck et al., Orthop Clin North Am, 2018; [9]Trentadue et al. J Orthop Res, 2024; [10]Cignoni et al., Euro Ital Chap, 2008, [11]Moerman, J Open Source Soft, 2018; [12]Suojarvi et al., Clin Anat, 2021; [13]Baumbach et al., BMC Med Imag, 2017;[14]Andreassen et al., arXiv, 2025; [15]Andreassen et al., Med Eng Phys, 2024; [16]Akoglu, Turk J Emerg Med, 2018;

ACKNOWLEDGEMENTS: The authors would like to thank the NIH for providing financial support through grants T32 AR056950, F31 AR082227, R01 AR071338, T32 GM065841, and T32 GM145408.

IMAGES AND TABLES:

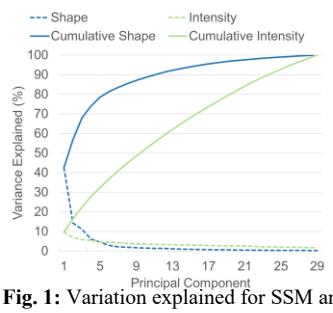

Fig. 1: Variation explained for SSM and SIM by principal component (PC).

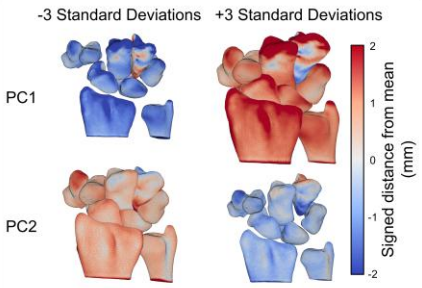

Fig. 2: SSM for ±3 standard deviation of the 1st and 2nd PCs. Colors are distance deformed outside (red) or inside (blue) of mean bones. Bones positioned at their mean centroids.

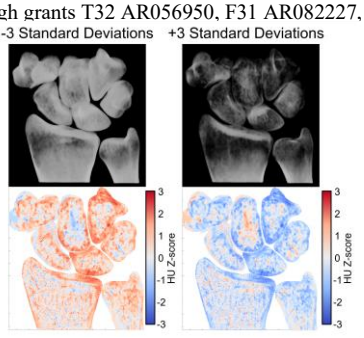

Fig. 3: SIM radiodensity maps for ±3 SD of 1st principal component of SIM. (*top*) Digitally reconstructed radiographs. (*bottom*) Increase (red) or decrease (blue) in radiodensity normalized to mean and standard deviation.